CAESIM

STORM Solver

VALIDATION / VERIFICATION REPORT

Adaptive Research

CONTENTS

SECTION **PAGE**

I. SOFTWARE DESCRIPTION

CAESIM is an advanced, general-purpose computational fluid dynamics (CFD) software system for simulating a wide range of fluid flow, heat transfer, and mass transfer problems including:

Subsonic, transonic, and supersonic flow regimes - Chemical reactions
Mutli-phase - Turbulence – Free Surface
Conjugate heat transfer – Porous media – Moving body treatment

The CAESIM software system is an integrated program suite providing the necessary tools for simulating real flows. The system includes modules for geometry creation and grid generation, a three-dimensional Navier-Stokes equation solver, and advanced visualization.

At the core of the system is a three-dimensional viscous flow solver that combines a strongly conservative finite-volume formulation with advanced features. Features such as collocated grids, high-order differencing schemes, and flexible user-accessible source code architecture produce a state-of -the-art CFD system that is powerful, efficient, and expandable.

Storm is fast, efficient, and accurate. The finite-volume treatment of the equations in general curvilinear coordinates produces accurate results on any smoothly varying grid even in the presence of significant non-orthogonality. By utilizing the integral form of the equations, conservation is enforced exactly. The PISO algorithm (pressure-implicit with splitting of operators) produces superior steady state and transient solutions.

II. VERIFICATION and VALIDATION PLAN

The purpose of the Verification and Validation Plan is to ensure that the CAESIM software performs its intended function.

The plan consists of two parts:

A. Testing the CAESIM software to solve known analytical and test case problems
B. Testing the CAESIM software against published experimental data

For Part A, three problems were selected and solved:

1. Radiation - Triangular Oven, Incropera F.P. & DeWitt D.P., Fundamentals of Heat Transfer, Chap. 13, pp. 660-664, John Wiley & Sons, 1981.
2. 1-D Conjugate Heat Transfer, analytical solution.
3. Free Convection in a Square Cavity, Davis, de Vahl and Jones, "Natural convection in a square cavity: a comparison exercise, Int. Journal for Numerical Methods in Fluids, 3, 1983.

For Part B, two problems were selected and solved:

4. Los Alamos Nuclear Storage Facility, Bernardin J.D. et al, CFD Analysis and experimental investigation associated with the design of the Los Alamos nuclear material storage facility, FEDSM '97, 1997.
5. Turbulent Circular Jet: 2-D Axisymmetric Analysis, Hinze J.O., Turbulence, Chap. 6, pp. 534-540, McGraw-Hill, 1975.

III. VERIFICATION and VALIDATION RESULTS

The results from the (5) selected CAESIM validation simulations are presented in the following sections. Individual write-ups and reference data are provided. All results compare favorably and confirm that CAESIM functions as designed.

Problem 1. Triangular Oven - Radiation

Introduction

Radiative heat transfer characteristics are studied for a paint brick oven in the form of a long triangular duct in which one surface is maintained at an elevated temperature and one other surface is insulated. Painted panels occupy the third surface and are maintained at a constant temperature. For validation purposes, the steady-state temperature of the insulated (i.e. adiabatic) surface is compared with an existing analytical solution [1].

Numerical Model

The numerical model is defined as follow:

- Flow Domain: 2-D Equilateral triangular cross-section, Side = 1m
  Grid of 2048 cells (64 cells along one side)

- Radiation Properties and Boundary Conditions

Side 1:	$\varepsilon = 0.8$, T = 1200 K (fixed temperature)
Side 2:	$\varepsilon = 0.4$, T = 500 K (fixed temperature)
Side 3:	$\varepsilon = 0.8$, Adiabatic surface (heat flux = 0)

The view factor model is used to predict radiative heat exchanges between the three surfaces of the triangular oven.

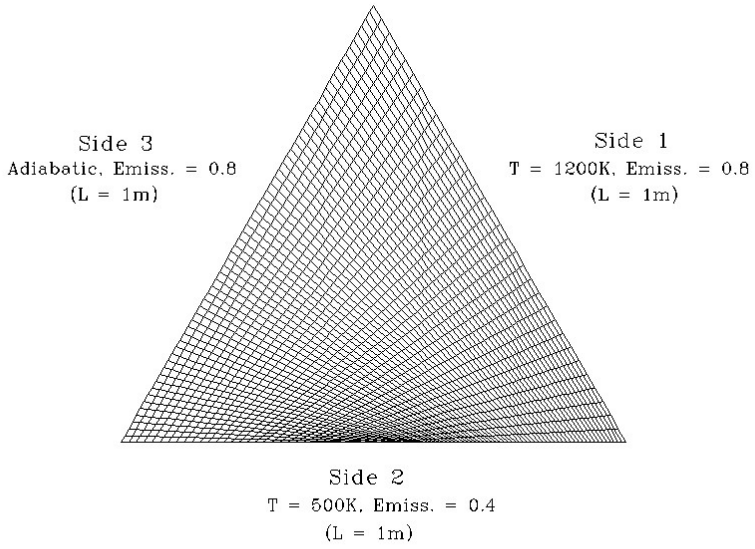

Figure 1. Numerical model – geometry, grid and boundary conditions.

Results

Based on the radiation properties of each side of the triangular oven, the analytical solution yields a temperature of 1102 K for the insulated surface. The figure below shows a comparison between the analytical value and the computed solution for the temperature along the insulated side of the equilateral triangle:

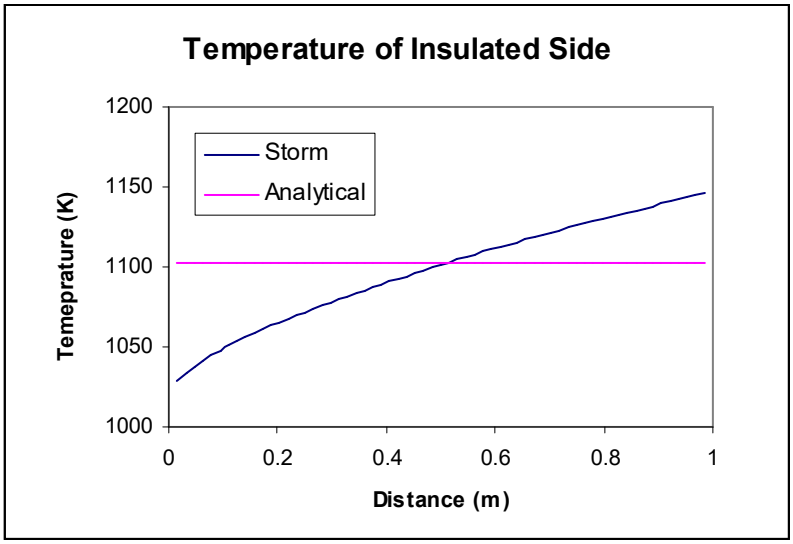

Figure 2. Comparison between numerical and analytical solutions.

Considering that one of the major assumptions to derive the analytical solution is to neglect end effects (i.e. constant temperature on the surface), the numerical results show excellent accuracy in predicting the average temperature on the insulated surface. They also demonstrate the influence of the end regions where the temperature is biased towards the constant value imposed on the adjacent side of the triangle (i.e. T = 500K at lower end and T = 1200K at higher end).

References

[1] Incropera F.P & DeWitt D.P., *Fundamentals of Heat Transfer*, Chap. 13, pp. 660-664, John Wiley & Sons, 1981.

Problem 2. 1-D Conjugate Heat Transfer

Introduction

Conjugate heat transfer exists when one (or more) fluid-solid interface is present in the computational domain. The simplest case of conjugate heat transfer occurs when only conduction is considered on both side of the fluid-solid interface. In this instance, the temperature distribution in the computational domain is dictated solely by the thermal conductivity of each material. If a one-dimensional temperature gradient is applied across the computational domain (i.e. fixed wall temperatures at opposite boundaries), the temperature distributions in both fluid and solid are linear with slopes inversely proportional to the ratio of the thermal conductivities.

Numerical Model

The numerical model is defined as follow:

Flow Domain:	1-D tube of length 2m (solid from x=0m to x=1m, fluid from x=1m to x=2m) Grid of 40 cells in x-dir. (20 solid cells + 20 fluid cells)
Fluid Properties (SI):	$\rho = 1$, $\mu = 1$, $c_p = 1$, $\beta = 1$ $k = 0.5$
Solid Properties (SI):	$\rho = 1$, $c_p = 1$ $k = 1$
Boundary Conditions:	u = 0 , T = 500K @ x = 0 u = 0 , T = 350K @ x = 2
Initial Conditions:	u = 0 , T_{solid} = 500K , T_{fluid} = 350K @ t = 0

For validation purposes, the thermal conductivity of the solid is twice the conductivity of the fluid so, based on the initial conditions, the temperature at the fluid-solid interface is expected to be 450K.

Note: to enforce pure conduction (i.e. no forced of free convection) in the fluid, only the energy (i.e. temperature) equation is solved.

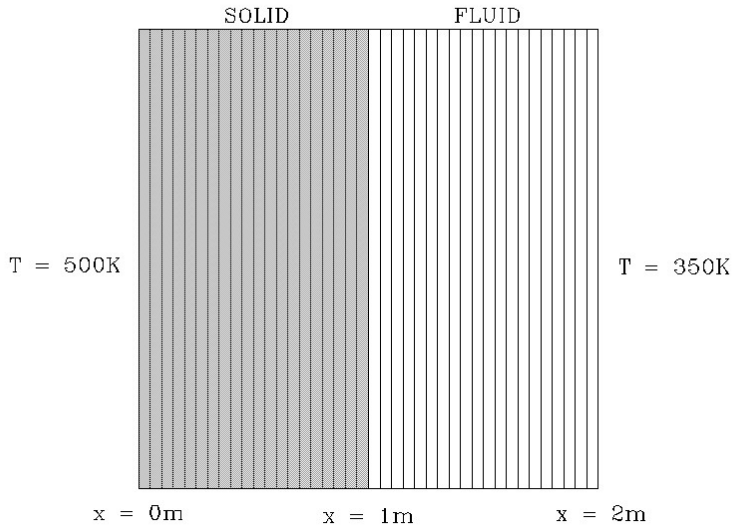

Figure 1. Numerical model - geometry, grid and boundary conditions.

Results

The numerical results are compared with the 1-D analytical solution based on the heat transfer balance at fluid-solid interface derived as follow:

$$k_f * (T_i - T_{f,w}) = k_s * (T_{s,w} - T_i)$$

where $T_{f,w}$ and $T_{s,w}$ are the temperature at the wall boundaries and T_i the temperature at the fluid-solid interface. k_f and k_s are the fluid and solid thermal conductivity. Solving for the temperature at the fluid-solid interface:

$$T_i = (k_s T_{s,w} + k_f T_{f,w}) / (k_s + k_f)$$

Introducing $T_{f,w} = 350K$, $T_{s,w} = 500K$ and $k_s = 2k_f$, the temperature at the interface becomes:

$$T_i = 450K$$

The numerical results replicate exactly the analytical solution as they show a temperature of 450K at the solid-fluid interface and slope change factor of 2 between the solid and the fluid materials.

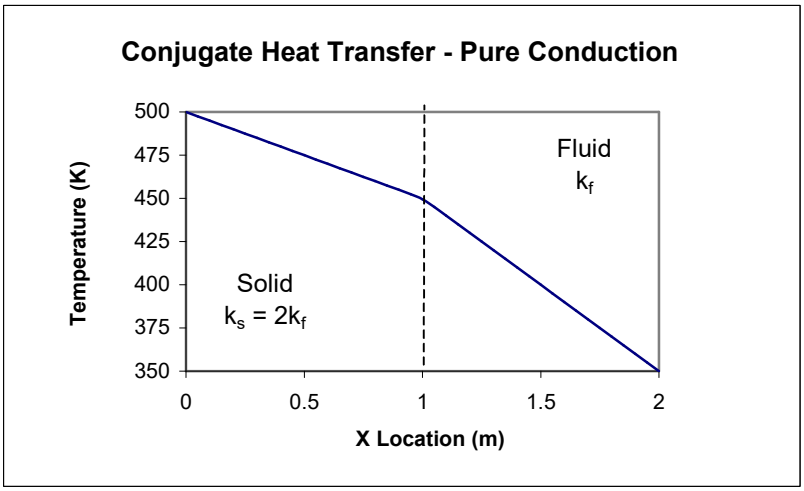

Figure 2. Temperature distribution in solid and fluid materials.

Problem 3. Free Convection in a Square Cavity

Introduction

In free convection, the flow is driven by temperature gradients small enough so that the Boussinesq approximation can be used for buoyancy forces. Free convection effects are characterized by a non-dimensional parameter, the Rayleigh number, representing the ratio of buoyancy forces and viscous forces:

$$Ra = \frac{\beta g \rho^2 C_p b^3 (T_1 - T_2)}{k\mu}$$

where $\beta = 1/T$ is the coefficient of volumetric expansion, g is gravity, ρ is density, Cp is the specific heat, b is the characteristic length (the size of the cavity), T_1 and T_2 are the characteristic temperatures that drive the buoyancy flow (left and right wall temperature, respectively), k is the conductivity of the fluid and μ is the viscosity.

Numerical Model

Using a non-dimensional formulation, the free convection flow is determined uniquely by the Rayleigh number with the characteristics of the numerical model defined as follow:

Flow Domain:	2-D square cavity of 1x1 dimensions Grid of 50x50 cells w/ clustering factor (1.6) near walls
Fluid Properties:	ρ = 1 μ = sqrt(Pr/Ra) (Prandtl number: Pr = 0.71) c_p = sqrt(Ra*Pr) (Prandtl number: Pr = 0.71) k = 1 β = 1
Boundary Conditions:	u = v = 0 , T = 0 @ x = 0 u = v = 0 , T = 1 @ x = 1 u = v = 0 , Flux = 0 @ y = 0 and y = 1
Initial Conditions:	u = v = 0 , T = 0 @ t = 0

For validation purposes, two different Rayleigh numbers (1,000 and 100,000) are simulated

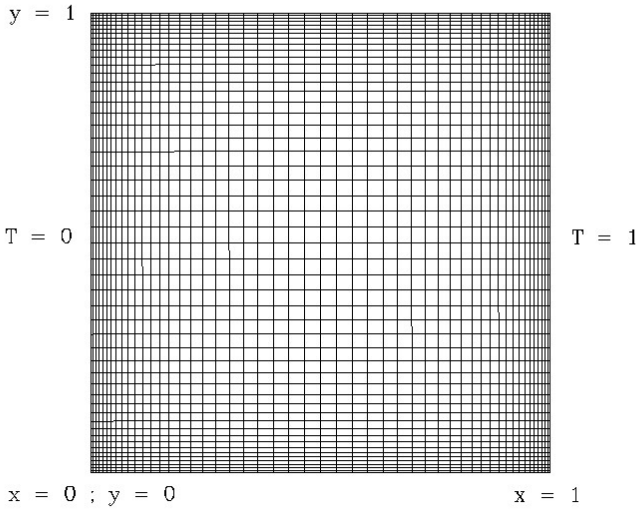

Figure 1. Numerical model – geometry, grid and boundary conditions.

Results

The results are presented in terms of the non-dimensional velocities and Nusselt number (non-dimensional heat transfer) defined as follow:

$$U^* = u^*U_{ref} \ , \ V^* = v^*U_{ref} \quad \text{where} \ U_{ref} = \text{sqrt}(Ra^*Pr)$$

U*max is defined as the maximum velocity in the x-direction at x = 0.5 and, similarly, V*max is the maximum velocity in the y-direction at y = 0.5.

The Nusselt number is defined as the non-dimensional temperature gradient in the x-direction at x = 0.98.

Ra = 1000	Storm	Davis	Relative Error
U^*_{max}	3.620	3.634	- 0.4 %
V^*_{max}	3.716	3.679	1.0 %
Nu_{max}	1.568	1.501	4.5 %
Nu_{min}	0.730	0.694	5.2 %

Table 1. Non-dimensional results comparison, Rayleigh number = 1,000

Ra = 100,000	Storm	Davis	Relative Error
U^*_{max}	34.07	34.81	- 0.3 %
V^*_{max}	68.67	68.22	1.0 %
Nu_{max}	7.797	7.761	0.5 %
Nu_{min}	0.735	0.736	- 0.1 %

Table 2. Non-dimensional results comparison, Rayleigh number = 100,000

The results for both Rayleigh numbers show excellent agreement with the reference data published by Davis [1]. Temperature contours and velocity vectors for both cases are presented in Appendix A.

Reference

[1] Davis, de Vahl and Jones, “Natural convection in a square cavity: a comparison exercise”, Int. Journal for Numerical Methods in Fluids, 3, 1983.

Appendix A

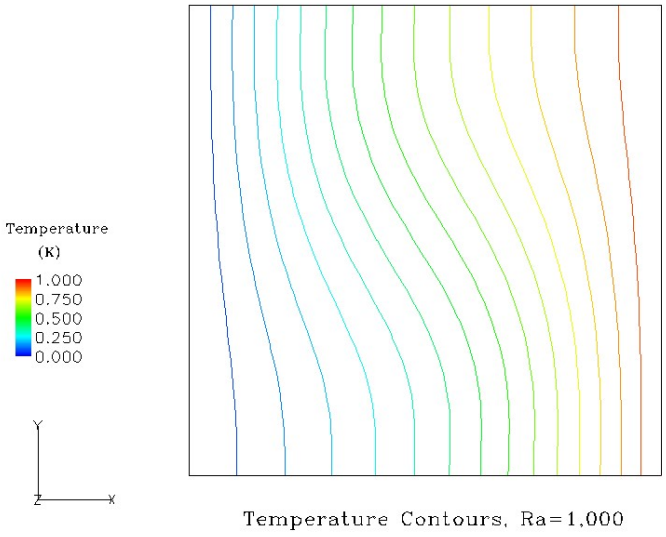

Figure A1. Temperature Contours, Ra = 1,000.

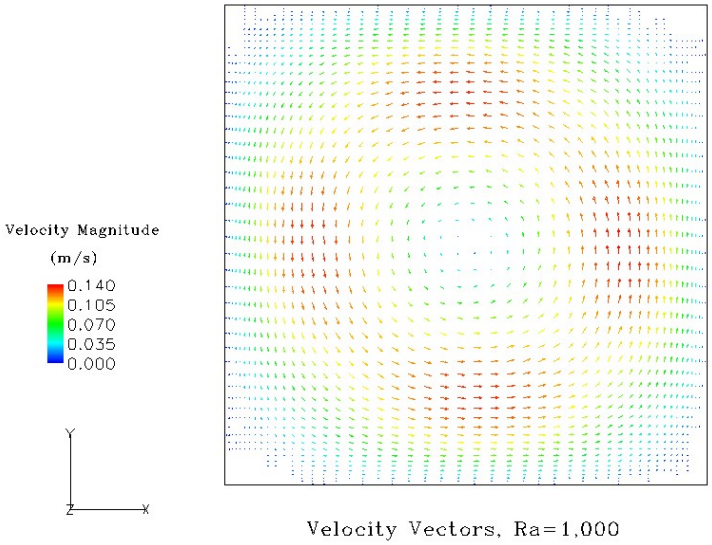

Figure A2. Velocity Vectors, Ra = 1,000.

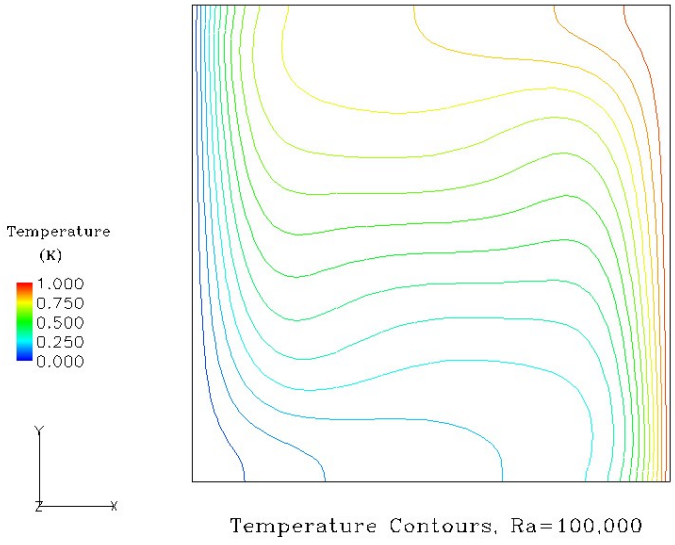

Figure A3. Temperature Contours, Ra = 100,000.

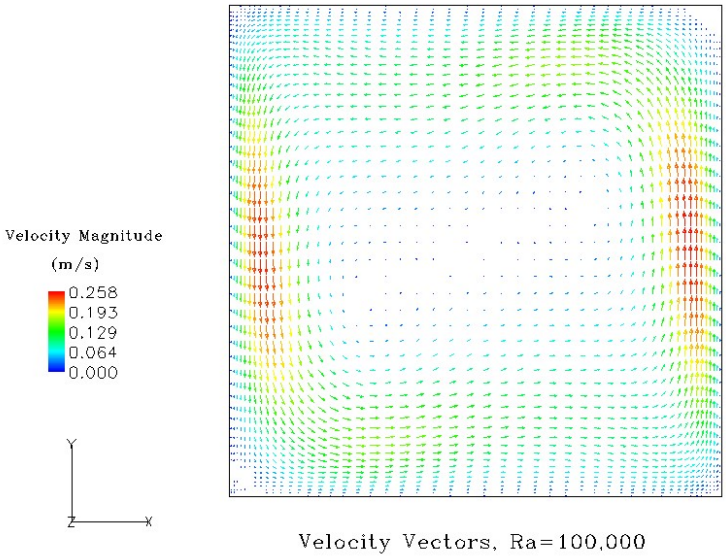

Figure A4. Velocity Vectors, Ra = 100,000.

Problem 4. Los Alamos Nuclear Storage Facility

Introduction

A detailed experimental study of the Los Alamos nuclear storage facility was performed in 1997 by Bernardin et al. [1] to assess the cooling efficiency of the airflow inside and outside a storage pipe that can hold 14 fuel canisters. Since each of the canisters is designed to generate at most 15W of thermal energy, the total heat dissipated by the nuclear fuel is 210W. The heat generated by the canisters induces a buoyant flow inside the storage pipe. The heat absorbed by the pipe from free convection and radiation will in turn drive a natural convection airflow on the outside of the storage unit. The pipe is also expected to loose heat to the outside walls of the facility through radiation.

Reproducing the entire geometry of the storage facility would be beyond the scope of this validation effort and therefore some simplifications were made to the numerical model. The main assumption is that for the non-forced airflow case as described in Bernardin et al., the problem can be treated as symmetric for a 90 degrees section of the canister and storage pipe. Also, while turbulent effects in the flow are taken into account with the use of a standard k-ε model, the influence of wall roughness is globally neglected. Preliminary work clearly demonstrated that the assumption of laminar flow is not accurate and turbulent regime has to be considered to properly model heat transfer characteristics. With the current modifications, the overall numerical solution is expected to produce qualitatively correct physical behavior, but may show slight discrepancies when compared directly to the results presented in the literature.

Numerical Model

After simplifications, the final geometry is a 90 degrees section of the original configuration with one side coincident to the vertical symmetry plane and the other one normal to it and through the center of the middle canister. The boundary conditions on

the two symmetry planes and on the outside wall have been adjusted to reproduce the free convection and radiation characteristics of the whole system. A complete description of the numerical model is given below:

- Flow Domain

Geometry:	Canister diameter = 0.127 m
	Storage pipe outer diameter = 0.457 m
	Storage pipe wall thickness = 0.013 m
	Storage pipe to outside wall distance = 0.0765 m
	Storage unit total height = 4.458 m

- Computational Grid

Radial direction:	10 (int. air) + 3 (pipe) + 6 (ext. air) = 19 cells
Circ. direction:	12 cells
Vertical direction:	50 cells
Total grid size:	19 x 12 x 50 = 11,400 cells

- Material Properties

Air:	Ideal gas law, Boussinesq approximation, Standard k-ε model
Storage Pipe:	Stainless steel

- Boundary Conditions

Canister wall:	heat flux = 118 W/m2, emissivity = 0.3, no slip
Storage pipe:	emissivity = 0.75, no slip
Outside wall:	emissivity = 0.1, no slip

- Initial Conditions

Internal air:	T = 310K, u = v = w = 0
External air:	T = 295K, u = v = w = 0

A view factor model is used to predict radiative heat exchanges between the different surfaces of the canister, storage pipe and outside wall.

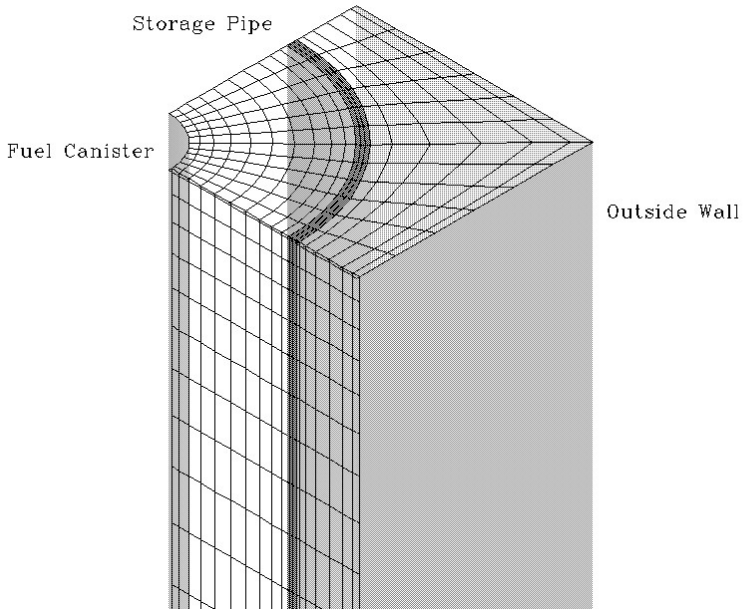

Figure 1. Numerical model – geometry and grid.

Results

The results are presented in terms of the vertical temperature distribution on the canister surface, in the internal air and in the storage pipe. They are compared with the experimental and numerical data reported in Bernardin et al. for their 1997 analysis of the Los Alamos nuclear materials storage facility.

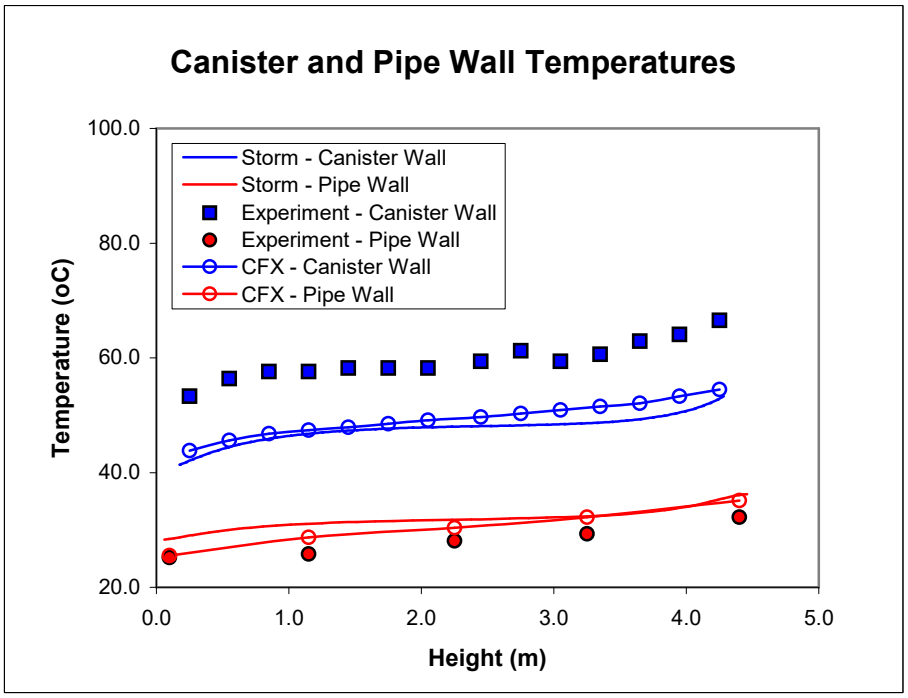

Figure 2. Comparison between numerical and experimental temperatures.

The results show a good agreement between the numerical simulations for the storage pipe walls. The discrepancies appearing on the canister surface temperatures have been documented by Bernardin et al. (c.f. Attachment I) and can be mainly attributed to slightly different heat inputs from the canisters between the numerical models and the experimental configuration:

"The differences in the numerical and experimental canister surface temperatures were discovered to lie in the method used to model the canister geometry. In the numerical model, the series of canisters was modeled as a continuous pipe with a uniform heat flux provided by 210W of input energy. While the same 210W was supplied to the canister in the experiment, the surface area over which the heat was dissipated was different than that used in the model since the canisters were separated by a 5.08cm (2.0in) gap. Assuming that the heat was dissipated solely by the outer side surface of the canisters in

*the experiment, then 20% less surface area would be available to dissipate the 210W of thermal energy in the experiment compared to the model. This indicates then that a 80% lower heat flux exists in the numerical model, and hence predicted canister surface temperatures would be significantly less than experimental values." (*Bernardin et al.)

Considering the assumptions and simplifications introduced in the numerical model, the results obtained with Storm demonstrate its ability to predict accurately the effects of combined free convection, conjugate and radiative heat transfer in a complex 3-D case.

Reference

Bernardin J.D. et al., CFD Analysis and experimental investigation associated with the design of the Los Alamos nuclear material storage facility, FEDSM'97, 1997.

Problem 5. Turbulent Circular Jet: 2-D Axismmetric Analysis

Introduction

The study of a turbulent circular jet issuing in a still ambient fluid has been the subject of many numerical and experimental investigation. A similarity solution for the flow rate in the wake of the jet is also available, which makes the jet analysis an excellent validation problem for high speed turbulent flows.

Numerical Model

Since the jet is circular, the assumption is made to treat the problem as 2-D axisymmetric and the geometry is simplified accordingly. Turbulent effects are accounted for by using a standard k-ε model.

- Flow Domain

Geometry:	2-D Axisymmetric region 1.0'' long by 0.1'' wide

- Computational Grid

Axial direction:	20 cells from z = 0.00'' to z = 0.15''
	40 cells from z = 0.15'' to z = 0.50''
	25 cells from z = 0.50'' to z = 1.00''
Radial direction:	64 cells
Circ. direction:	axisymmetric (i.e. 1 cell)
Total grid size:	(20+40+25) x 64 = 5440 cells

- Fluid Properties

Water:	$\rho = 1000$ kg/m^3 , $\mu = 8.0e^{-4}$ m^2/s
	Standard k-ε turbulence model

- Inlet Boundary Conditions

Velocity:	Uz = 101.5 m/s, Ur = 0 m/s
Turbulence:	k = 0.02 m^2/s^2, ε = 0.02 m^2/s^3

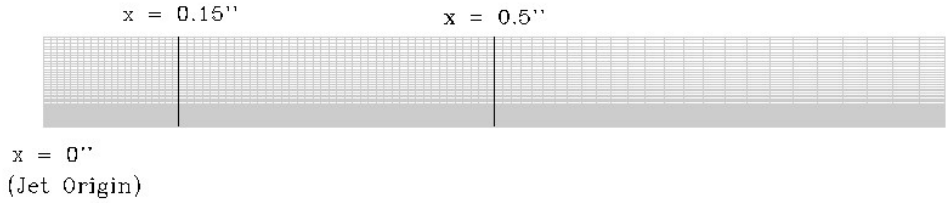

Figure 1. Numerical model – geometry and grid.

Results

The results are presented in terms of the flow rate for the self-preserving region of the wake and of normalized velocity profiles across the jet in the radial direction. Theses values can be directly compared to analytical and experimental results for axisymmetric wall jets reported in the literature [1].

- Flow Rate for Self-preserving Region

Flow rate from similarity: $Q_z = 0.32*Q_d*z/d$

Where $Q_d = 10$ cc/min
$d = 0.0018$ in

Axial Location (in)	**Flow Rate CAESIM** (cc/min)	**Flow Rate Similarity** (cc/min)	**Relative Error** (%)
0.15	249	267	6.7
0.50	933	889	4.9

Table 1. Flow rates for self-preserving wake region.

- Normalized Velocity Profiles

Normalized Jet Velocity: $U^* = U_z / U_{z,max}$
Normalized Jet Radius: $r^* = r / z$

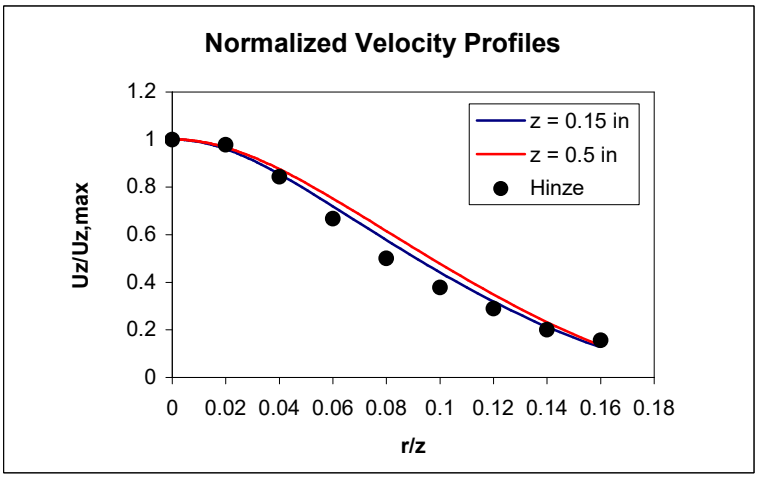

Figure 1. Normalized velocity profile across jet.

Reference

[1] Hinze J.O., *Turbulence*, Chap. 6, pp. 534-540, McGraw-Hill, 1975.

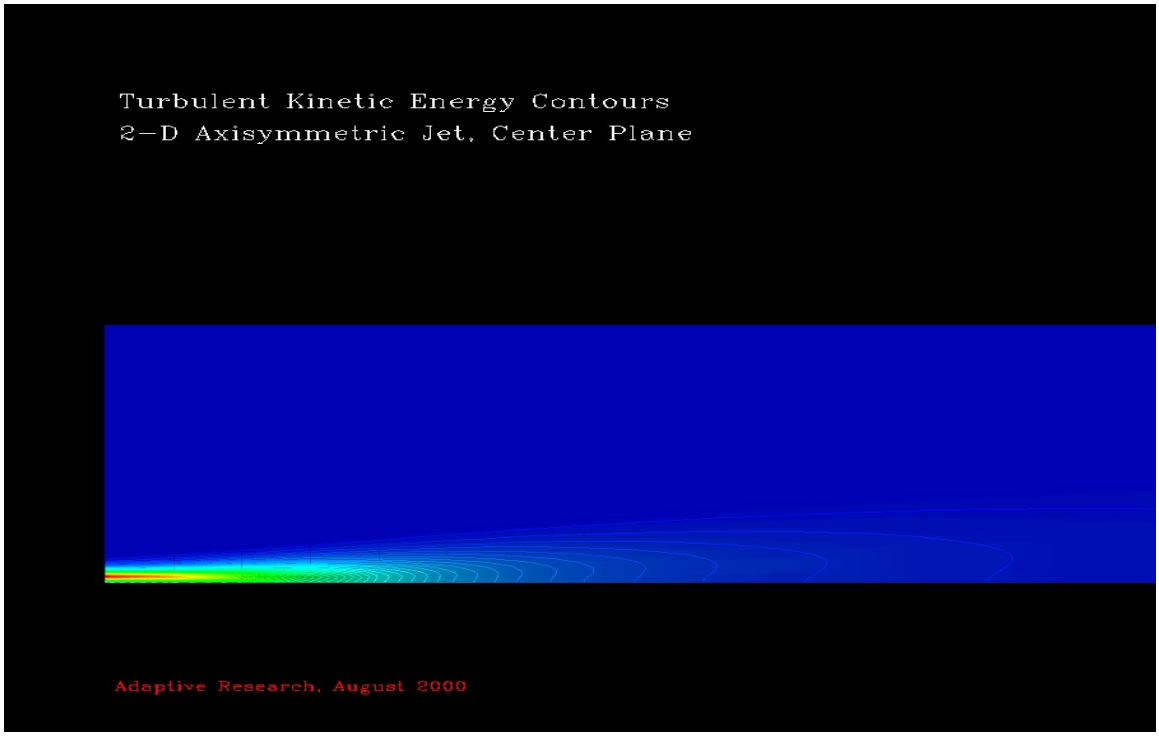

Turbulent kinetic energy contours for axisymmetric jet.